Physiological regulation of epithelial tight junctions is associated with myosin light-chain phosphorylation

JERROLD R. TURNER,[1,2] BRIAN K. RILL,[2] SUSAN L. CARLSON,[1] DENISE CARNES,[1] RACHEL KERNER,[1] RANDALL J. MRSNY,[3] AND JAMES L. MADARA[1]
[1]*Division of Gastrointestinal Pathology, Department of Pathology, Brigham and Women's Hospital and the Harvard Digestive Disease Center, Boston, Massachusetts 02115;* [2]*Department of Pathology, Harper Hospital and the Karmanos Cancer Institute, Wayne State University, Detroit, Michigan 48201; and* [3]*Department of Pharmaceutical Research and Development, Genentech Incorporated, South San Francisco, California 94080*

Turner, Jerrold R., Brian K. Rill, Susan L. Carlson, Denise Carnes, Rachel Kerner, Randall J. Mrsny, and James L. Madara. Physiological regulation of epithelial tight junctions is associated with myosin light-chain phosphorylation. *Am. J. Physiol.* 273 (*Cell Physiol.* 42): C1378–C1385, 1997.—Tight junctions serve as the rate-limiting barrier to passive movement of hydrophilic solutes across intestinal epithelia. After activation of Na^+-glucose cotransport, the permeability of intestinal tight junctions is increased. Because previous analyses of this physiological tight junction regulation have been restricted to intact mucosae, dissection of the mechanisms underlying this process has been limited. To characterize this process, we have developed a reductionist model consisting of Caco-2 intestinal epithelial cells transfected with the intestinal Na^+-glucose cotransporter, SGLT1. Monolayers of SGLT1 transfectants demonstrate physiological Na^+-glucose cotransport. Activation of SGLT1 results in a $22 \pm 5\%$ fall in transepithelial resistance (TER) ($P < 0.001$). Similarly, inactivation of SGLT1 by addition of phloridzin increases TER by $24 \pm 2\%$ ($P < 0.001$). The increased tight junction permeability is size selective, with increased flux of small nutrient-sized molecules, e.g., mannitol, but not of larger molecules, e.g., inulin. SGLT1-dependent increases in tight junction permeability are inhibited by myosin light-chain kinase inhibitors (20 μM ML-7 or 40 μM ML-9), suggesting that myosin regulatory light-chain (MLC) phosphorylation is involved in tight junction regulation. Analysis of MLC phosphorylation showed a 2.08-fold increase after activation of SGLT1 ($P < 0.01$), which was inhibited by ML-9 ($P < 0.01$). Thus monolayers incubated with glucose and myosin light-chain kinase inhibitors are comparable to monolayers incubated with phloridzin. ML-9 also inhibits SGLT1-mediated tight junction regulation in small intestinal mucosa ($P < 0.01$). These data demonstrate that epithelial cells are the mediators of physiological tight junction regulation subsequent to SGLT1 activation. The intimate relationship between tight junction regulation and MLC phosphorylation suggests that a critical step in regulation of epithelial tight junction permeability may be myosin ATPase-mediated contraction of the perijunctional actomyosin ring and subsequent physical tension on the tight junction.

permeability; intestine; sodium-glucose cotransport

INTESTINAL EPITHELIAL CELLS orchestrate selective absorptive and secretory processes and serve as barriers that restrict the passive transepithelial movement of hydrophilic solutes. The ability of such solutes to passively traverse lipid membranes is limited; thus the major pathway for hydrophilic solute permeation across epithelial monolayers is paracellular. The intercellular tight junction, or zonula occludens, serves as the rate-limiting barrier that restricts solute movement through the paracellular pathway. For example, the permeability characteristics of tight junctions do not appear to be invariant but may be regulated by a variety of agonists, both acutely and chronically (7, 15, 16, 22). Second, it has been observed that tight junctions display an array of proteins enriched at, or specifically localized to, this site. These include an integral membrane protein, occludin, which may mediate the tight junction sealing function (36), and cytosolic peripheral membrane proteins, with a domain structure suggesting protein-protein linking function, e.g., ZO-1 and ZO-2 (9, 28). In addition, small cytosolic GTPases, including Rab 13, Rab 3B, and Rho (22, 38) and nonmembrane tyrosine kinases (29), may directly regulate tight junction protein interactions. Lastly, tight junctions are in close apposition to a circumferential ring of actin and myosin II, which are arranged to permit contractile/tension responses that may influence tight junction permeability via mechanical means (1, 17–19, 33). Although most microfilament-membrane associations at this latter site appear to occur at the adherens junction, just below the tight junction, microfilaments also appear to intimately associate with the plasma membrane within tight junctions at membrane "kiss" sites, the anatomic sites where membranes of adjacent cells are in closest apposition. These kisses are the sites at which many tight junction-specific proteins localize and also correspond to the fibrils recognized in freeze-fracture images of tight junctions.

Mechanistic studies of acute regulation of tight junction permeability in cell culture systems have generally used agonists under conditions that do not correspond directly to physiological events. Thus, although these data yield important insights, it is difficult to assess the physiological relevance of the molecular events that have been described. In contrast, physiological regulation of tight junction permeability has been described in the small intestine. Here, it has been demonstrated that activation of the Na^+-glucose cotransporter, SGLT1, on the apical membrane of epithelial cells leads to increased tight junction permeability for small solutes. The altered tight junction permeability is accompanied by morphological modifications of the tight junctions and condensation of perijunctional actin-myosin II rings (1, 19). Unfortunately, biochemical studies of tight junction regulation in small intestines have been

prohibited by the structural complexity, limited ability to be manipulated ex vivo, and cellular heterogeneity of such tissues.

Cell culture models of intestinal epithelial monolayers might lend themselves to biochemical analysis of physiological SGLT1-mediated tight junction regulation. Unfortunately, currently available polarized intestinal epithelial cell models that display biophysical confluence requisite for analyses of tight junctions express only low levels of SGLT1. To circumvent this problem, we have recently shown that, whereas only trace SGLT1-like surface activity is expressed by the human intestinal epithelial cell line Caco-2, stable transfection of the SGLT1 protein in these cells is accompanied by markedly enhanced surface expression (32). This SGLT1 expression is appropriately apically polarized and exhibits predicted substrate binding characteristics and sensitivity to selective inhibitors. Furthermore, monolayers of the transfected cells demonstrate transepithelial Na^+-glucose cotransport comparable to that observed in natural epithelia (32).

In these epithelial monolayers, SGLT1 activation leads to modifications of tight junction permeability similar to those previously demonstrated in natural intestinal epithelia. This regulation is inhibited by the myosin light-chain kinase inhibitors ML-7 and ML-9 (8, 24). SGLT1 activation and associated increases in tight junction permeability are paralleled by phosphorylation of myosin light chain, suggesting that activation of SGLT1 results in enhanced cytoskeletal tension and myosin light-chain phosphorylation. Similar to its effect on SGLT1-mediated tight junction regulation, ML-9 also inhibited myosin light-chain phosphorylation. Thus we conclude that myosin light-chain phosphorylation and resultant increases in cytoskeletal tension may be critical events in physiological regulation of intestinal epithelial tight junctions.

METHODS

Cell culture and transfection. Clone BBe Caco-2 cells were kindly provided by Dr. M. Mooseker (23) and grown in high-glucose Dulbecco's modified Eagle's medium (Life Technologies, Gaithersburg, MD) supplemented with 10% fetal calf serum (FCS) and 15 mM *N*-2-hydroxyethylpiperazine-*N*′-2-ethanesulfonic acid (HEPES), pH 7.4. Before transfection, the cells were passaged before becoming confluent.

For growth as polarized monolayers, Transwell inserts (Corning-Costar, Cambridge, MA) were coated with rat tail collagen as previously described (20). Caco-2 cells from a nearly confluent flask were trypsinized to a single cell suspension and plated onto inserts at a final surface area dilution of 1:8. Medium in these cultures was replaced thrice weekly. To allow for the Caco-2 cells to differentiate as absorptive enterocytes, monolayers were typically used between 20 and 30 days after plating.

Electrophysiology. Electrophysiological measurements were made with agar bridges and Ag-AgCl calomel electrodes as previously described (20). Potential differences were measured before and during application of a 50-μA current. Transepithelial short-circuit current (I_{sc}) and transepithelial resistance (TER) were calculated with Ohm's law. Monolayers were transferred from culture medium to Hanks' balanced salt solution (HBSS) with 15 mM HEPES, pH 7.4, and 25 mM D-glucose. For monolayers incubated with phloridzin, 25 mM glucose was replaced by 5 mM glucose, 20 mM mannitol, and 2 mM phloridzin. The myosin light-chain kinase inhibitors ML-9 (40 μM; Molecular Probes, Eugene, OR) or ML-7 (20 μM; Calbiochem, La Jolla, CA) were included in HBSS with 25 mM D-glucose.

Mannitol and inulin flux studies. Monolayers grown on 12-mm-diameter Snapwell supports were used with a vertical diffusion chamber system (Corning-Costar) for analysis of transepithelial solute flux. Monolayers were mounted in HBSS with 15 mM HEPES, pH 7.4, 1 mM inulin, 2.5 mM mannitol and either 25 or 5 mM D-glucose, 20 mM L-glucose, and 2 mM phloridzin. After 90 min of incubation, 5 μCi of [^{3}H]mannitol (New England Nuclear), from a 250 μCi/ml stock in 90% ethanol, and 1 μCi of [^{14}C]inulin (New England Nuclear), from a 50 μCi/ml stock in water, were added to the apical chamber of each monolayer. Aliquots were removed from the basal chamber after 0, 20, 40, 60, and 80 min and replaced with equal volumes of the identical buffer. After correction for volumes removed, interval fluxes were calculated, using specific activities determined individually for each chamber. Flux rates were stable over the four intervals examined. Mean flux rate for each monolayer was used for statistical analyses.

Ex vivo studies of hamster intestinal mucosae. These were performed as previously described (1). Briefly, male golden hamsters weighing 180–220 g were anesthetized with pentobarbital sodium (Nembutal), and the small intestine was rapidly removed. After the serosa and external longitudinal layer of the muscularis propria were stripped away, sheets were placed in Ussing chambers equipped with calomel voltage-sensitive electrodes and Ag-AgCl current-passing electrodes. Mucosal and serosal sides of the chamber were attached to circulating 10-ml chambers equilibrated with 95% O_2-5% CO_2 maintained at 37°C. The mucosal buffer contained the high-oxygen affinity perfluorochemical Oxypherol-ET (20% wt/vol) as previously described (19). The serosal chamber also contained 3 mM glucose, which was balanced osmotically with 3 mM mannitol in the mucosal chamber. After a 25-min equilibration period, baseline transmucosal resistance was measured with Ohm's law by measuring the voltage deflection elicited by a 100-μA current (1 s). Transmucosal resistance was recorded as the total resistance minus the resistance of the bathing solutions. In experiments using ML-9, the drug (50 μM) was included during the initial equilibration. After measurement of baseline resistance, 20 mM glucose (with or without 50 μM ML-9) or 20 mM mannitol was added to mucosal and serosal chambers, respectively. Transmucosal resistance was measured 20 min after addition of the sugar.

Quantitative analysis and ^{32}P labeling of myosin light chain. For ^{32}P-labeling experiments, monolayers were grown on 1.0-cm^2-surface area Transwell inserts. These were preequilibrated in phosphate-free Eagle's minimum essential medium (Life Technologies) supplemented with 15 mM HEPES (pH 7.4), 20 mM mannitol, and 1% dialyzed FCS (Sigma Chemical, St. Louis, MO) containing 250 μCi/ml of [^{32}P]phosphoric acid (New England Nuclear) for 2 h. Monolayers were then transferred to test medium (phosphate-free HBSS) with 250 μCi/ml of [^{32}P]phosphoric acid and 25 mM glucose, 25 mM glucose and 40 μM ML-9, or 5 mM glucose, 20 mM mannitol, and 2 mM phloridzin for 2 h. At the end of this time, inserts were washed three times in cold phosphate-buffered saline (PBS) and scraped into 50 μl of lysis buffer [150 mM NaCl, 50 mM tris(hydroxymethyl)aminomethane (pH 8), 0.02% NaN_3, 1% Nonidet P-40, 0.1% sodium dodecyl sulfate (SDS), 0.5% sodium deoxycholate, 6 mM phenylmeth-

ylsulfonyl fluoride, 2 μg/ml aprotinin, 20 μg/ml chymostatin]. Samples (10 μl) were separated on 15% SDS-polyacrylamide gel electrophoresis (PAGE) gels as previously described (14) and transferred to Immobilon (Millipore, Bedford, MA) polyvinylidene difluoride membranes by standard methods (31). After transfer, membranes were blocked in PBS with 10% normal goat serum (Sigma) for 1 h at 4°C. After blocking was completed, membranes were washed in PBS for 1 min, washed in methanol for 30 s, and allowed to dry for 2 h at room temperature.

Membranes were marked with an autoradiography pen (Sigma) exposed in a PhosphorImager exposure screen, and the cassette was imaged on a model 425E PhosphorImager (Molecular Dynamics, Sunnyvale, CA). The density of these bands was quantified using ImageQuant software (Molecular Dynamics). Membranes were then rehydrated in PBS with 10% normal goat serum for 5 min at room temperature and incubated with monoclonal anti-myosin light-chain antibody (clone MY-21, Sigma) diluted 1:4,000 overnight at 4°C. After five washes in PBS with 5% normal goat serum, membranes were incubated with affinity-purified peroxidase-conjugated goat anti-mouse antisera (ICN Cappel, Costa Mesa, CA) at 2 μg/ml for 2 h at room temperature. Membranes were then washed five times in PBS with 5% normal goat serum and once in PBS, prepared for enhanced chemiluminescence according to the manufacturer's instructions (Amersham, Arlington Heights, IL), and exposed with preflashed Biomax MR film (Eastman Kodak, Rochester, NY). Preliminary experiments using immunoprecipitated whole myosin from the same cell extracts showed that only one of the bands identified by immunoblotting with MY-21 was immunoprecipitated with myosin heavy chains. Furthermore, the additional two bands detected were variably present over multiple experiments. Recovery of myosin regulatory light chain (MLC) from immunoprecipitates was variable. Thus a whole cell lysate analysis was employed. Films were scanned with a personal densitometer (Molecular Dynamics), and band densities were quantified with ImageQuant software. Preliminary experiments demonstrated that the immunoblot-chemiluminescence signal intensity was linear over a range of MLC loads. Relative phosphorylation was calculated as the ^{32}P band density per immunoblot band density. In each experiment, these values were normalized to the mean relative phosphorylation of monolayers incubated with 5 mM glucose, 20 mM mannitol, and 2 mM phloridzin.

Statistics. Means of multiple measurements and standard deviations were calculated in each case. Comparisons were made with a one-tailed *t*-test.

RESULTS

Caco-2 cell lines stably transfected with SGLT1 were used for these studies. We have previously shown that the Michaelis-Menten constant for sugar uptake, the rate constant for Na^+ uptake, and the Hill coefficient for Na^+ uptake of these cells are similar to previously reported values for SGLT1-mediated Na^+-glucose cotransport (32). Analysis of uptake of the SGLT1-specific glucose analog [^{14}C]methyl α-glucoside in polarized monolayers of SGLT1-transfected Caco-2 cells verified that SGLT1 was correctly sorted and expressed primarily on the apical surface of transfected Caco-2 cells (32). In addition, after correction for mucosal surface area, these monolayers showed physiological range small intestinal TER, low basal I_{sc} in the absence of Na^+-nutrient cotransport, and electrogenic SGLT1-mediated Na^+-glucose cotransport (Table 1).

SGLT1-transfected Caco-2 cells have lower TER when SGLT1 is active. The initial goal of these studies was to develop an in vitro system of Na^+-glucose-dependent tight junction regulation comparable with that documented in mammalian small intestinal mucosae. Because glucose is an essential nutrient for these cells, rather than eliminate it from the medium entirely we inactivated apical SGLT1-mediated Na^+-glucose cotransport selectively with phloridzin. Phloridzin competes for the sugar binding site of SGLT1 and thus serves as a specific inhibitor of SGLT1-mediated Na^+-glucose cotransport. Because phloridzin does not inhibit basolateral facilitated glucose transport via the glucose transporter isoform GLUT-2, the cells are not nutrient deprived. After 18 h of culture in medium with phloridzin, TER values of four separate subclones of SGLT1-transfected Caco-2 monolayers increased, ranging from 123 ± 14% to 138 ± 16% of the TER of matched monolayers incubated without phloridzin (Fig. 1). In contrast, TER of identically prepared monolayers of nontransfected Caco-2 cells incubated for 18 h in medium with phloridzin was not significantly different from that of matched monolayers incubated without phloridzin (Fig. 1). These data indicate that increased TER in response to phloridzin in SGLT1-expressing clones is due to inhibition of active SGLT1-mediated Na^+-glucose cotransport.

Acute regulation of tight junction resistance in SGLT1 transfectants. An SGLT1-transfected Caco-2 clone with reproducible increases in TER after 18 h culture with phloridzin and a 39-fold enhancement of SGLT1-mediated methyl α-glucoside uptake, relative to nontransfected Caco-2 clones, was used for the majority of these studies (32). However, results were similar with other clones stably transfected with SGLT1. To characterize regulation of TER by Na^+-glucose-mediated activation of transfected SGLT1, we measured the TER of

Table 1. *Electrophysiology of monolayers of SGLT1-transfected and nontransfected Caco-2 cell clones*

	TER, Ω·cm²	Basal I_{sc} (Inactive SGLT1), μA/cm²	Glucose-Induced I_{sc} (Active SGLT1), μA/cm²
SGLT1-transfected Caco-2	136 ± 10	2.3 ± 0.3	4.4 ± 0.6
Nontransfected Caco-2	120 ± 46	1.3 ± 0.2	1.0 ± 0.5

Values are means ± SD. Monolayers of subcloned intestinal Na^+-glucose cotransporter (SGLT1)-transfected Caco-2 cells and subcloned nontransfected Caco-2 cells were cultured on 0.33-cm² Transwell chambers as described. Clones with similar physiological range small intestinal transepithelial resistance (TER) were compared. Measurement of transepithelial short-circuit current (I_{sc}) in the presence of 2 mM phloridzin, 5 mM glucose, and 20 mM mannitol showed similar basal I_{sc} in the cell lines. In contrast, removal of phloridzin and mannitol in exchange for 25 mM glucose resulted in marked augmentation of I_{sc} in SGLT1-transfected, but not nontransfected, cell monolayers. These data ($n = 3$) show that SGLT1-transfected monolayers express physiological transepithelial Na^+ transport mediated via SGLT1 and are typical of many subclones of both transfected and nontransfected Caco-2 cells.

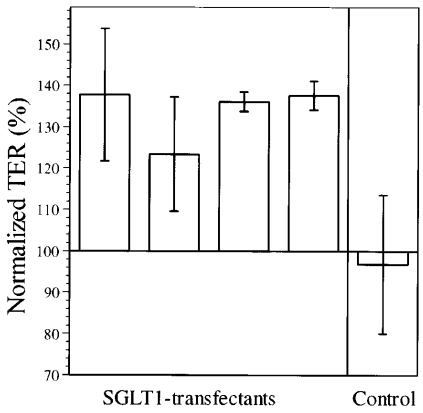

Fig. 1. Transepithelial resistance (TER) of Caco-2 monolayers after 18 h of inhibition of the intestinal Na^+-glucose cotransporter (SGLT1). Monolayers of 4 Caco-2 clones transfected independently with SGLT1 and monolayers of nontransfected Caco-2 clones (control) were transferred to culture medium with or without 2 mM phloridzin (to inhibit SGLT1). After 18 h of incubation, monolayers were transferred to Hanks' balanced salt solution (HBSS) with or without phloridzin and TER was measured. These data are representative of many similar experiments. SGLT1-transfected cell monolayers typically demonstrated 25–35% increases in TER after incubation with phloridzin. Significant differences between nontransfected monolayers incubated with or without phloridzin were not observed.

phloridzin-treated, SGLT1-transfected Caco-2 monolayers after washout of the phloridzin and addition of 25 mM glucose. As shown in Fig. 2*A*, activation of SGLT1 by removal of phloridzin and addition of 25 mM glucose resulted in a 22 ± 5% decrease in TER ($P < 0.001$). This decrease in TER was complete within 2 h and was similar in magnitude to the changes shown in Fig. 1. This decrease in TER is also similar in magnitude to the decreased resistance induced by addition of apical glucose to intestinal segments isolated from fasted rodents (1, 19). In contrast to the SGLT1-transfected Caco-2 cell monolayers, no significant TER response was noted in monolayers of nontransfected Caco-2 cells exposed to identical conditions (data not shown).

We also characterized TER increases following acute inhibition of SGLT1-mediated Na^+-glucose cotransport by the addition of phloridzin (Fig. 2*B*). Inhibition of SGLT1 activation resulted in a 24 ± 2% increase in TER ($P < 0.001$). The time course of this increase in TER was more prolonged than that of TER decreases following SGLT1 activation but was complete within 2–2.5 h. These data show that Na^+-glucose cotransport-dependent regulation of TER is reversible in SGLT1-transfected Caco-2 monolayers. Similar reversibility has been demonstrated in isolated mammalian intestinal mucosa and corresponds to the "resetting" of tight junction permeability that must occur when Na^+-cotransported nutrients are removed from the lumen.

Analysis of the kinetics of TER regulation in SGLT1 transfectants showed that the rate of TER decrease on acute activation of SGLT1-mediated Na^+-glucose cotransport was greater than the rate of TER increase following acute inhibition of SGLT1. The best-fit straight line for the TER decrease when SGLT1 is activated over 0–60 min had a slope of 24 $\Omega \cdot cm^2 \cdot h^{-1}$, whereas the slope of the line fit to the TER increase over the first 60 min after SGLT1 inhibition was 13 $\Omega \cdot cm^2 \cdot h^{-1}$. Similarly, the time required to achieve a half-maximal change in TER was ~60 min for the SGLT1 activation-dependent TER decrease but was ~90 min for the TER increase following SGLT1 inhibition. Such findings suggest that modest differences may exist in the "on" and "off" rates of the SGLT1 activation-dependent TER responses.

Regulation of tight junction resistance correlates with altered tight junction size selectivity. To verify that changes in TER are due to altered tight junction permeability, transepithelial flux of [^{3}H]mannitol and [^{14}C]inulin in glucose- and phloridzin-treated monolayers of SGLT1-transfected Caco-2 cells was measured. As shown in Fig. 3, the transepithelial flux of mannitol (hydrodynamic radius of 3.6 Å) was 7.93 ± 0.65 $nmol \cdot cm^{-2} \cdot h^{-1}$ in glucose-treated monolayers but was only 5.23 ± 0.51 $nmol \cdot cm^{-2} \cdot h^{-1}$ in phloridzin-treated

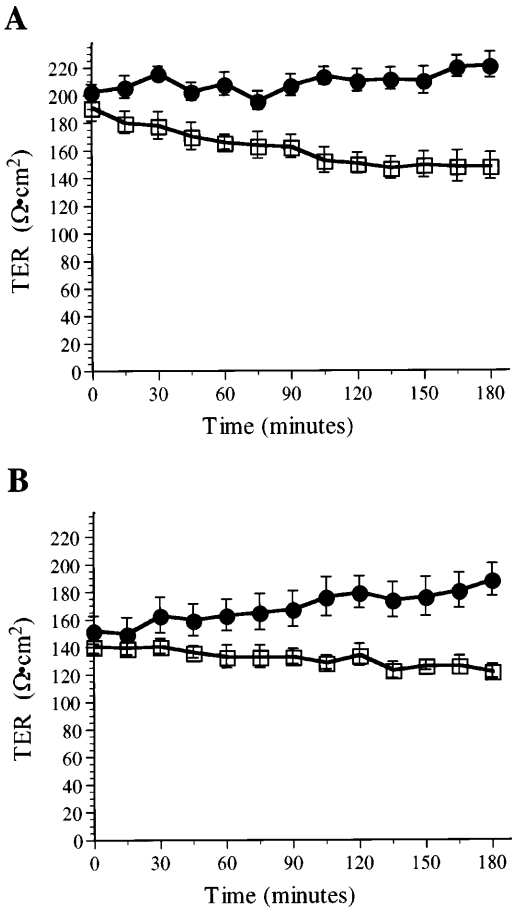

Fig. 2. Kinetics of Na^+-glucose cotransport-dependent TER regulation. *A*: TER decreases rapidly following activation of Na^+-glucose cotransport. SGLT1-transfected Caco-2 monolayers were incubated for 15 h in culture medium with 0.5 mM phloridzin. They were then transferred to HBSS with either 25 mM glucose (□) or 5 mM glucose, 20 mM mannitol, and 2 mM phloridzin (●). Data are typical of many experiments. Data are means ± SD, $n = 6$. *B*: TER increases following inhibition of Na^+-glucose cotransport. SGLT1-transfected Caco-2 monolayers were incubated for 15 h in culture medium with 25 mM glucose. They were then transferred to HBSS with either 25 mM glucose (□) or 5 mM glucose, 20 mM mannitol, and 2 mM phloridzin (●). Data are typical of many experiments. Data are means ± SD, $n = 6$.

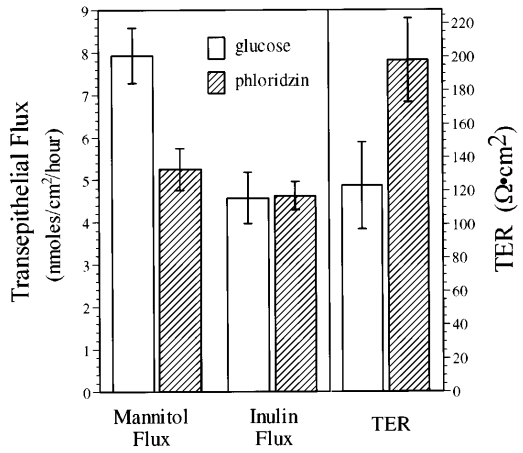

Fig. 3. Changes in transepithelial flux parallel Na^+-glucose cotransport-dependent changes in TER. Monolayers of SGLT1-transfected Caco-2 cells were mounted in diffusion chambers with either HBSS with 25 mM D-glucose or HBSS with 5 mM D-glucose, 20 mM L-glucose, and 2 mM phloridzin. Both solutions contained 1 mM inulin and 2.5 mM mannitol. After equilibration, trace [^{3}H]mannitol and [^{14}C]inulin were added to the apical side of each monolayer. Transepithelial flux of these markers was determined, and TER was measured as described. Data are means ± SD, $n = 6$.

monolayers, a difference of 34% ($P < 0.001$). This change paralleled the increase in TER from 123 ± 26 to 198 ± 25 $\Omega \cdot cm^2$ following phloridzin treatment, a difference of 38% ($P < 0.001$). In contrast to mannitol, the transepithelial flux of inulin (hydrodynamic radius of 11.5 Å) was similar in glucose- and phloridzin-treated monolayers, 4.57 ± 0.60 and 4.62 ± 0.33 $nmol \cdot cm^{-2} \cdot h^{-1}$, respectively ($P = 0.86$). These data show that the SGLT1-dependent changes in TER are due to altered tight junction permeability and that the alterations in tight junction permeability are both regulated and size selective. Furthermore, the size selectivity of these alterations verifies that TER changes are due to tight junction regulation and cannot be due to perturbations such as those associated with cell shedding, cell death, or other artifacts.

MLC phosphorylation is increased in glucose-treated SGLT1-transfected Caco-2 cell monolayers. Indirect data have suggested that one means of regulating intestinal epithelial tight junction permeability is via mechanical tension exerted by the cytoskeleton (33). Ultrastructural analyses of mammalian intestinal mucosa exhibiting altered tight junction permeability following SGLT1 activation are consistent with this hypothesis (1, 19). Monolayers of SGLT1-transfected Caco-2 clones in which Na^+-glucose cotransport regulates tight junction permeability provide an opportunity to test this hypothesis. Phosphorylation of the 20-kDa regulatory light chain of myosin II (MLC) has been shown to positively regulate actomyosin contraction in numerous cell types (2, 4, 10, 30), including the brush border of the enterocyte (2, 3, 11, 12, 35). To determine whether MLC phosphorylation occurs as a consequence of intestinal Na^+-glucose cotransport, we evaluated monolayers of ^{32}P-labeled SGLT1-transfected Caco-2 cells. As shown in Fig. 4, SDS-PAGE analysis identified three phosphoproteins with molecular masses of ~20 kDa. Comparisons of the autoradiograph either with anti-myosin light-chain immunoblots (Fig. 4) or with immunoprecipitated myosin light chain identified one of these bands as MLC. We assessed phosphorylation of the MLC band in whole cell lysates by normalizing the ^{32}P signal intensity to that of a quantitative immunoblot of the same SDS-PAGE gel. These analyses demonstrated a 2.08-fold increase in MLC phosphorylation in SGLT1-transfected Caco-2 monolayers with active Na^+-glucose cotransport relative to identical monolayers incubated with phloridzin (Fig. 4; $P < 0.01$). These data demonstrate that MLC phosphorylation occurs during Na^+-glucose cotransport-dependent tight junction regulation and are consistent with previous demonstrations of morphological cytoskeletal condensation in isolated intestinal mucosa.

Inhibition of myosin light-chain kinase prevents both MLC phosphorylation and SGLT1-initiated decreases in TER. Although the data presented above demonstrate that Na^+-glucose cotransport simultaneously results in increased tight junction permeability and MLC phosphorylation, we sought to demonstrate a direct relationship between these events. We used the myosin light-chain kinase inhibitors ML-7 and ML-9 to prevent actomyosin contraction (8, 24). These inhibitors are structurally similar but differ in their inhibition constant values for myosin light-chain kinase, protein kinase A, and protein kinase C (24). As shown in Fig. 5*A*, 20 μM ML-7 or 40 μM ML-9 were similar in their ability to nearly completely inhibit the decrease in TER after activation of Na^+-glucose cotransport. After 2 h of incubation, in 25 mM glucose with 20 μM ML-7 or 25 mM glucose with 40 μM ML-9, TER values were 97 ± 2% or 101 ± 2% of the TER of monolayers incubated with phloridzin. These TER values were significantly different from that of monolayers incubated in 25 mM glucose without myosin light-chain kinase inhibitors ($P < 0.01$ for glucose vs. either glucose + ML-7 or glucose + ML-9) but were not significantly different from the TER of monolayers

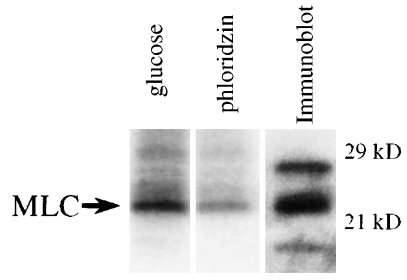

Fig. 4. Myosin regulatory light chain (MLC) is phosphorylated following Na^+-glucose cotransport in SGLT1-transfected Caco-2 monolayers. MLC phosphorylation was assessed in lysates of ^{32}P-labeled monolayers after 2 h of incubation in HBSS with 25 mM glucose or HBSS with 5 mM glucose, 20 mM mannitol, and 2 mM phloridzin. Samples were separated on 15% SDS-polyacrylamide gel electrophoresis. After autoradiography (left 2 lanes), the MLC band was detected by quantitative immunoblot (right lane is representative) to provide both localization of MLC and measurement of MLC content for each sample. Autoradiograph signal for each MLC band was normalized to the quantitative immunoblot intensity for that band to control for variation in the MLC loaded.

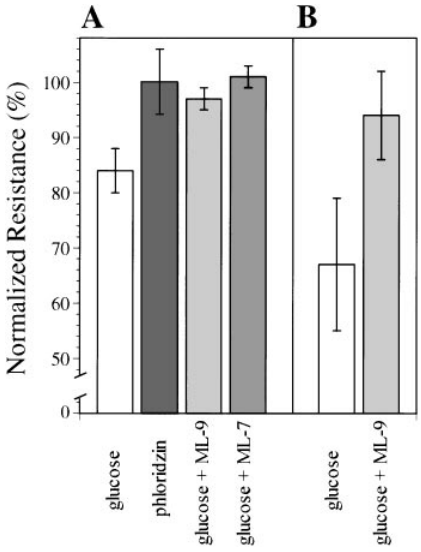

Fig. 5. Na^+-glucose cotransport-dependent regulation of resistance is blocked by myosin light-chain kinase inhibitors. *A*: ML-9 and ML-7 inhibit Na^+-glucose cotransport-dependent TER regulation in SGLT1-transfected Caco-2 monolayers. Monolayers were transferred from medium to HBSS with 25 mM glucose, 5 mM glucose-20 mM mannitol with 2 mM phloridzin, 25 mM glucose with 40 μM ML-9, or 25 mM glucose with 20 μM ML-7. TER values were normalized to the mean TER of the monolayers incubated with phloridzin. Data are means ± SD, $n = 3$. *B*: ML-9 inhibits Na^+-glucose cotransport-dependent transmucosal resistance regulation in isolated mammalian small intestinal mucosa. Transmucosal resistance was measured after 25 min of equilibration. Glucose (20 mM) with or without 50 μM ML-9 was then added to the mucosal reservoir, and mannitol (20 mM) was added to the serosal reservoir. Data for each chamber were normalized to the starting transmucosal resistance for that chamber. Data are means ± SD, $n = 7$.

incubated with phloridzin. In some, but not all, experiments, phloridzin and ML-9 together effected a small increase in TER relative to phloridzin alone that was neither additive nor statistically significant.

Quantitative analysis of MLC phosphorylation in monolayers after incubation with 25 mM glucose and 40 μM ML-9 was only 0.53-fold greater than that of monolayers incubated with phloridzin. This increase was significantly different from the 2.08-fold increase in MLC phosphorylation in monolayers incubated with glucose without ML-9 ($P < 0.01$) but was not significantly different from MLC phosphorylation in monolayers incubated with phloridzin.

Limitations in ex vivo viability of mammalian intestinal mucosae as well as the presence of multiple cell types in such preparations prevent direct analyses of MLC phosphorylation in response to SGLT1 activation. However, such preparations can be used with short preincubations of myosin light-chain inhibitors and thus can be used to verify that inhibition of myosin light-chain kinase also prevents Na^+-glucose cotransport-dependent tight junction regulation in natural mucosa. The transmucosal resistance of isolated hamster mucosal sheets mounted in Ussing chambers and incubated with 25 mM glucose fell to 67 ± 12% of the starting transmucosal resistance (Fig. 5*B*). In contrast, the inclusion of ML-9 resulted in a final transmucosal resistance that was 94 ± 8% of the starting transmucosal resistance ($P < 0.01$). These data suggest that the molecular pathways that mediate Na^+-glucose cotransport-dependent regulation of tight junctions in SGLT1-transfected Caco-2 cells reflect those that are operative in mammalian small intestine.

DISCUSSION

In this study, we have detailed the creation and characterization of a cell culture model of physiological tight junction regulation. We have used this model to evaluate physiological regulation of epithelial tight junctions at the molecular level. This has not been possible previously because of the absence of physiological tight junction regulation in cultured cell monolayers and the complexities of using intact mucosae for this purpose. We developed our model using the BBe clone of the Caco-2 cell line, which differentiates with an intestinal absorptive enterocyte phenotype and possesses a well-developed apical brush border (23). This clone was transfected with the intestinal Na^+-glucose cotransporter SGLT1 (32). Monolayers of the resulting transfectants demonstrated physiological Na^+-glucose cotransport-dependent tight junction regulation typical of that which occurs in mammalian small intestinal mucosae. We have shown that, after activation of Na^+-glucose cotransport in these cell monolayers, MLC phosphorylation occurs in concert with increased tight junction permeability. Further evidence that this is not merely a coincidental correlation is the fact that inhibitors of myosin light-chain kinase similarly block increases in MLC phosphorylation and increases in tight junction permeability, both in cultured monolayers and in intact mucosae. These data suggest a direct link between MLC phosphorylation and physiological intestinal tight junction regulation.

The intimate relationship between intestinal epithelial tight junctions and the apical cytoskeleton has been previously demonstrated (3, 17–20). The apical cytoskeleton contains a prominent perijunctional actomyosin ring (PAMR) that is capable of generating contractile force. For example, PAMR contraction, and associated myosin phosphorylation, can effect rounding of the apical surface (2). The application of such lateral tension to the tight junction can lead to ultrastructural deformations of epithelial tight junctions, and disassembly of the PAMR can result in markedly increased tight junction permeability (7, 18, 22). The observation that ultrastructural condensation of the PAMR occurred in conjunction with Na^+-nutrient cotransport-dependent increases in tight junction permeability led to the hypothesis that increased cytoskeletal tension on the tight junction may be a mediator in physiological regulation of epithelial tight junction permeability (1, 33). Unfortunately, detailed analysis of this process is not technically feasible in intact mucosae. Thus biochemical studies of physiological tight junction regulation have not been previously possible.

A role for MLC phosphorylation in tight junction regulation has been suggested in other epithelial models. For example, in intestinal epithelial cells, MLC phosphorylation occurs after colonization with entero-

pathogenic *E. coli* (37). Reorganization of the apical cytoskeleton and increased tight junction permeability occur in parallel with this MLC phosphorylation (26). Although these observations represent important precedents for the regulation of epithelial tight junctions, Na^+-nutrient cotransport-dependent tight junction regulation differs significantly from enteropathogenic *E. coli*.-induced changes in permeability in that the former is more rapid, is reversible, and is a tightly regulated process with size-selective increases in tight junction permeability. In addition, expression of a constitutively active myosin light-chain kinase in a renal epithelial cell line, Madin-Darby canine kidney cells, results in the formation of monolayers with TER values that are $<10\%$ of control monolayers (6).

Phosphorylation of MLC has been implicated in regulation of endothelial permeability following stimulation with thrombin, histamine, or adenosine 3′,5′-cyclic monophosphate (5, 21). This phenomenon has been studied extensively, since it results in well-defined cytoskeletal contraction with retraction of endothelial cells (21). These events lead to the development of spaces between endothelial cells and increased endothelial permeability to macromolecules. Kinetic analyses have shown that endothelial MLC phosphorylation occurs after an increase in intracellular Ca^{2+} but before the development of cytoskeletal tension (5). This temporal sequence supports the hypothesis that elevation of intracellular Ca^{2+} leads to activation of myosin light-chain kinase that, in turn, results in MLC phosphorylation and subsequent cytoskeletal contraction. However, in contrast to intestinal epithelium, endothelial cytoskeletal contraction leads to physical cell separation and the development of macromolecular intercellular gaps.

Although intermediate events in the physiological regulation of intestinal epithelial permeability may be similar to those for endothelial contraction, i.e., MLC phosphorylation, both initial stimuli and ultimate effects are distinctly different. The in vivo trigger for endothelial contraction, inflammation, is typically a long-lived phenomenon whose development is facilitated by macromolecular intercellular gaps. In contrast, the development of macromolecular gaps in the intestine would severely compromise maintenance of the mucosal barrier. Accordingly, whereas permeability to small nutrient-sized molecules, e.g., mannitol, is increased, that of larger molecules, e.g., inulin, remains unchanged. Thus modulation of intestinal permeability is precisely regulated with respect to size selectivity and does not include gross cellular retraction, as occurs in endothelial cells. The primary in vivo stimulus in intestinal epithelium, the presence of luminal nutrients, is an event that repeats itself relatively frequently; thus the resulting increases in intestinal permeability must be reversible within a short time. Although the process is reversible, the kinetics of increased vs. decreased tight junction permeability differ. The role of MLC phosphorylation may explain this difference between the rate of Na^+-glucose cotransport-dependent decreases in TER, 24 $\Omega \cdot cm^2 \cdot h^{-1}$, and the rate of TER increase, 13 $\Omega \cdot cm^2 \cdot h^{-1}$, after inhibition of Na^+-glucose cotransport. These data would be consistent with rapid MLC phosphorylation after activation of myosin light-chain kinase and slower MLC dephosphorylation after myosin light-chain kinase inactivation. Alternatively, the differing kinetics may reflect more rapid activation, relative to inactivation, of myosin light-chain kinase itself or differences in activation and inactivation rates for SGLT1.

MLC phosphorylation represents only one mechanism of rapid tight junction regulation. Other potential mechanisms, including phosphorylation of the tight junction protein ZO-1, have been described (13, 27, 34). Although these mechanisms have phosphorylation events in common, the specific kinases involved are likely different, since MLC phosphorylation typically occurs on serine and threonine residues (4), whereas ZO-1 is phosphorylated on tyrosine residues (13, 34). Nonetheless, signaling systems proximal to kinase activation, for example elevation of intracellular Ca^{2+}, may ultimately lead to both MLC and ZO-1 phosphorylation. As yet undefined phosphorylation events are also critical in tight junction assembly (25) and thus may contribute to long-term tight junction regulation. The relationship between these events and other potential mechanisms of long-term tight junction regulation, including recruitment of junction components and expression of differing ZO-1 isoforms, is presently unknown.

In summary, we have established a unique in vitro cell culture system for the study of Na^+-nutrient cotransport-dependent regulation of intestinal permeability. Using this cultured cell system, we have, for the first time, demonstrated a relationship between MLC phosphorylation and physiological regulation of intestinal epithelial permeability. It is anticipated that further use of this model system will allow identification and characterization of additional intracellular events in Na^+-nutrient cotransport-dependent regulation of intestinal permeability that both precede and follow MLC phosphorylation.

We thank Drs. John Pappenheimer, Daniel Louvard, Monique Arpin, Sylvie Robin, Ernie Wright, Gail Hecht, Wayne Lencer, Sunil Shaw, and Tucker Collins for their helpful and supportive interactions during various phases of this work.

This work was supported by National Institute of Diabetes and Digestive and Kidney Diseases Grants DK-35932 (J. L. Madara) and DK-02503 (J. R. Turner), Individual National Research Service Award DK-09180 (J. R. Turner), the Harvard Digestive Diseases Center Grant P01-DK-34854, the Wayne State University School of Medicine Fund for Medical Research and Education, and in part by Genentech.

This work was presented in preliminary form at the annual meeting of the American Gastroenterological Association, Washington, DC, 1997.

Present address of J. L. Madara: Dept. of Pathology, Emory University School of Medicine, 1364 Clifton Rd., Atlanta, GA 30322.

Address for reprint requests: J. R. Turner, Dept. of Pathology, Wayne State Univ. School of Medicine, 540 E. Canfield, Detroit, MI 48201.

Received 11 April 1997; accepted in final form 24 June 1997.

REFERENCES

1. **Atisook, K., S. Carlson, and J. L. Madara.** Effects of phlorizin and sodium on glucose-elicited alterations of cell junctions in intestinal epithelia. *Am. J. Physiol.* 258 (*Cell Physiol.* 27): C77–C85, 1990.

2. **Broschat, K. O., R. P. Stidwill, and D. R. Burgess.** Phosphorylation controls brush border motility by regulating myosin structure and association with the cytoskeleton. *Cell* 35: 561–571, 1983.
3. **Burgess, D. R.** Reactivation of intestinal epithelial cell brush border motility: ATP-dependent contraction via a terminal web contractile ring. *J. Cell Biol.* 95: 853–863, 1982.
4. **Colburn, J. C., C. H. Michnoff, L. C. Hsu, C. A. Slaughter, K. E. Kamm, and J. T. Stull.** Sites phosphorylated in myosin light chain in contracting smooth muscle. *J. Biol. Chem.* 263: 19166–19173, 1988.
5. **Goeckeler, Z. M., and R. B. Wysolmerski.** Myosin light chain kinase-regulated endothelial cell contraction: the relationship between isometric tension, actin polymerization, and myosin phosphorylation. *J. Cell Biol.* 130: 613–627, 1995.
6. **Hecht, G., L. Pestic, G. Nikcevic, A. Koutsouris, J. Tripuraneni, D. D. Lorimer, G. Nowak, V. Guerriero, Jr., E. L. Elson, and P. D. Lanerolle.** Expression of the catalytic domain of myosin light chain kinase increases paracellular permeability. *Am. J. Physiol.* 271 (*Cell Physiol.* 40): C1678–C1684, 1996.
7. **Hecht, G., C. Pothoulakis, J. T. Lamont, and J. L. Madara.** *Clostridium difficile* toxin A perturbs cytoskeletal structure and tight junction permeability of cultured human intestinal epithelial monolayers. *J. Clin. Invest.* 56: 1053–1061, 1988.
8. **Ishikawa, T., T. Chijiwa, M. Hagiwara, S. Mamiya, M. Saitoh, and H. Hidaka.** ML-9 inhibits the vascular contraction via the inhibition of myosin light chain phosphorylation. *Mol. Pharmacol.* 33: 598–603, 1988.
9. **Jesaitis, L. A., and D. A. Goodenough.** Molecular characterization and tissue distribution of ZO-2, a tight junction protein homologous to ZO-1 and the *Drosophila* discs-large tumor suppressor protein. *J. Cell Biol.* 124: 949–961, 1994.
10. **Kamm, K. E., and J. T. Stull.** Activation of smooth muscle contraction: relation between myosin phosphorylation and stiffness. *Science* 232: 80–82, 1986.
11. **Keller, T. C. D., K. A. Conzelman, R. Chasan, and M. S. Mooseker.** Role of myosin in terminal web contraction in isolated intestinal epithelial brush borders. *J. Cell Biol.* 100: 1647–1655, 1985.
12. **Keller, T. C. D., and M. S. Mooseker.** Ca^{2+}-calmodulin-dependent phosphorylation of myosin, and its role in brush border contraction in vitro. *J. Cell Biol.* 95: 943–959, 1982.
13. **Kurihara, H., J. M. Anderson, and M. G. Farquhar.** Increased Tyr phosphorylation of ZO-1 during modification of tight junctions between glomerular foot processes. *Am. J. Physiol.* 268 (*Renal Fluid Electrolyte Physiol.* 37): F514–F524, 1995.
14. **Laemmli, U. K.** Cleavage of structural proteins during the assembly of the head of bacteriophage T4. *Nature* 227: 680–685, 1970.
15. **Li, C. X., and M. J. Poznansky.** Effect of FCCP on tight junction permeability and cellular distribution of ZO-1 protein in epithelial (MDCK) cells. *Biochim. Biophys. Acta* 1030: 297–300, 1990.
16. **Madara, J. L.** Effects of cytochalasin D on occluding junctions of intestinal absorptive cells: further evidence that the cytoskeleton may influence paracellular permeability and junctional charge selectivity. *J. Cell Biol.* 102: 2125–2136, 1986.
17. **Madara, J. L.** Intestinal absorptive cell tight junctions are linked to cytoskeleton. *Am. J. Physiol.* 253 (*Cell Physiol.* 22): C171–C175, 1987.
18. **Madara, J. L., R. Moore, and S. Carlson.** Alteration of intestinal tight junction structure and permeability by cytoskeletal contraction. *Am. J. Physiol.* 253 (*Cell Physiol.* 22): C854–C861, 1987.
19. **Madara, J. L., and J. R. Pappenheimer.** Structural basis for physiological regulation of paracellular pathways in intestinal epithelia. *J. Membr. Biol.* 100: 149–164, 1987.
20. **Madara, J. L., J. Stafford, D. Barenberg, and S. Carlson.** Functional coupling of tight junctions and microfilaments in T84 monolayers. *Am. J. Physiol.* 254 (*Gastrointest. Liver Physiol.* 17): G416–G423, 1988.
21. **Moy, A. B., S. S. Shasby, B. D. Scott, and D. M. Shasby.** The effect of histamine and cyclic adenosine monophosphate on myosin light chain phosphorylation in human umbilical vein endothelial cells. *J. Clin. Invest.* 92: 1198–1206, 1993.
22. **Nusrat, A., M. Giry, J. R. Turner, S. P. Colgan, C. A. Parkos, D. Carnes, E. Lemichez, P. Boquet, and J. L. Madara.** Rho protein regulates tight junctions and perijunctional actin organization in polarized epithelia. *Proc. Natl. Acad. Sci. USA* 92: 10629–10633, 1995.
23. **Peterson, M. D., and M. S. Mooseker.** Characterization of the enterocyte-like brush border cytoskeleton of the C2BBe clones of the human intestinal cell line, Caco-2. *J. Cell Sci.* 102: 581–600, 1992.
24. **Saitoh, M., T. Ishikawa, S. Matsushima, M. Naka, and H. Hidaka.** Selective inhibition of catalytic activity of smooth muscle myosin light chain kinase. *J. Biol. Chem.* 262: 7796–7801, 1987.
25. **Singer, K. L., B. R. Stevenson, P. L. Woo, and G. L. Firestone.** Relationship of serine/threonine phosphorylation/dephosphorylation signaling to glucocorticoid regulation of tight junction permeability and ZO-1 distribution in nontransformed mammary epithelial cells. *J. Biol. Chem.* 269: 16108–16115, 1994.
26. **Spitz, J., R. Yuhan, A. Koutsouris, C. Blatt, J. Alverdy, and G. Hecht.** Enteropathogenic *Escherichia coli* adherence to intestinal epithelial monolayers diminishes barrier function. *Am. J. Physiol.* 268 (*Gastrointest. Liver Physiol.* 31): G374–G379, 1995.
27. **Stevenson, B. R., J. M. Anderson, I. D. Braun, and M. S. Mooseker.** Phosphorylation of the tight-junction protein ZO-1 in two strains of Madin-Darby canine kidney cells which differ in transepithelial resistance. *Biochem. J.* 263: 597–599, 1989.
28. **Stevenson, B. R., J. D. Siliciano, M. S. Mooseker, and D. A. Goodenough.** Identification of ZO-1: a high molecular weight polypeptide associated with the tight junction (zonula occludens) in a variety of epithelia. *J. Cell Biol.* 103: 755–766, 1986.
29. **Takeda, H., and S. Tsukita.** Effects of tyrosine phosphorylation on tight junctions in temperature-sensitive v-src-transfected MDCK cells. *Cell Struct. Funct.* 20: 387–393, 1995.
30. **Takeda, M., T. Homma, M. D. Breyer, N. Horiba, R. L. Hoover, S. Kawamoto, I. Ichikawa, and V. Kon.** Volume and agonist-induced regulation of myosin light-chain phosphorylation in glomerular mesangial cells. *Am. J. Physiol.* 264 (*Renal Fluid Electrolyte Physiol.* 33): F421–F426, 1993.
31. **Towbin, H., T. Staehelin, and J. Gordon.** Electrophoretic transfer of proteins from polyacrylamide gels to nitrocellulose sheets: procedure and some applications. *Proc. Natl. Acad. Sci. USA* 76: 4350–4354, 1979.
32. **Turner, J. R., W. I. Lencer, S. Carlson, and J. L. Madara.** Carboxy-terminal vesicular stomatitis virus G protein-tagged intestinal Na^+-dependent glucose cotransporter (SGLT1): maintenance of surface expression and global transport function with selective perturbation of transport kinetics and polarized expression. *J. Biol. Chem.* 271: 7738–7744, 1996.
33. **Turner, J. R., and J. L. Madara.** Physiological regulation of intestinal epithelial tight junctions as a consequence of Na(+)-coupled nutrient transport. *Gastroenterology* 109: 1391–1396, 1995.
34. **Van Itallie, C. M., M. S. Balda, and J. M. Anderson.** Epidermal growth factor induces tyrosine phosphorylation and reorganization of the tight junction protein ZO-1 in A431 cells. *J. Cell Sci.* 108: 1735–1742, 1995.
35. **Wolenski, J. S., S. M. Hayden, P. Forscher, and M. S. Mooseker.** Calcium-calmodulin and regulation of brush border myosin-I MgATPase and mechanochemistry. *J. Cell Biol.* 122: 613–621, 1993.
36. **Wong, V., and B. M. Gumbiner.** A synthetic peptide corresponding to the extracellular domain of occludin perturbs the tight junction permeability barrier. *J. Cell Biol.* 136: 399–409, 1997.
37. **Yuhan, R., A. Koutsouris, and G. Hecht.** Enteropathogenic *E. coli*-induced phosphorylation of myosin light chain increases intestinal epithelial paracellular permeability (Abstract). *Gastroenterology* 108: A948, 1995.
38. **Zahraoui, A., G. Joberty, M. Arpin, J. J. Fontaine, R. Hellio, A. Tavitian, and D. Louvard.** A small rab GTPase is distributed in cytoplasmic vesicles in nonpolarized cells but colocalizes with the tight junction marker ZO-1 in polarized epithelial cells. *J. Cell Biol.* 124: 101–115, 1994.